Structural Engineering and Mechanics, *Vol. 67, No. 2 (2018) 105-113*
DOI: https://doi.org/10.12989/sem.2018.67.2.105

A new model approach to predict the unloading rock slope displacement behavior based on monitoring data

Ting Jiang[1,2,3], Zhenzhong Shen[1,2,3], Meng Yang*[1,2,3], Liqun Xu[1,2,3], Lei Gan[1,2,3] and Xinbo Cui[4]

[1]State Key Laboratory of Hydrology-Water Resources and Hydraulic Engineering, Hohai University, Nanjing 210098, China
[2]College of Water Conservancy and Hydropower Engineering, Hohai University, Nanjing 210098, China
[3]National Engineering Research Center of Water Resources Efficient Utilization and Engineering Safety, Hohai University, Nanjing 210098, China
[4]Information Center of Land and Resources, Binzhou City, Binzhou, China

(Received May 9, 2018, Revised June 20, 2018, Accepted June 21, 2018)

Abstract. To improve the prediction accuracy of the strong-unloading rock slope performance and obtain the range of variation in the slope displacement, a new displacement time-series prediction model is proposed, called the fuzzy information granulation (FIG)-genetic algorithm (GA)-back propagation neural network (BPNN) model. Initially, a displacement time series is selected as the training samples of the prediction model on the basis of an analysis of the causes of the change in the slope behavior. Then, FIG is executed to partition the series and obtain the characteristic parameters of every partition. Furthermore, the later characteristic parameters are predicted by inputting the earlier characteristic parameters into the GA-BPNN model, where a GA is used to optimize the initial weights and thresholds of the BPNN; in the process, the numbers of input layer nodes, hidden layer nodes, and output layer nodes are determined by a trial method. Finally, the prediction model is evaluated by comparing the measured and predicted values. The model is applied to predict the displacement time series of a strong-unloading rock slope in a hydropower station. The engineering case shows that the FIG-GA-BPNN model can obtain more accurate predicted results and has high engineering application value.

Keywords: unloading rock slope; displacement prediction; fuzzy information granulation; genetic algorithm; back propagation neural network

1. Introduction

Owing to geological activities and engineering construction, there are widespread unloading rock slopes around the world. Many slopes are a result of human activities. In the event of failures and landslides, lives and property may be lost. Therefore, it is necessary to study the slope stability in order to convey it to the relevant personnel to take appropriate measures over time using limited monitoring and investigation data (Nieuwenhuis *et al.* 1991, Su *et al.* 2016, Chen *et al.* 2016, Yang *et al.* 2017a, Zhang *et al.* 2017). In recent years, in order to analyze and predict the rock slope behavior, many scholars have focused on mechanical models and intelligent mathematical models. Mechanical models probe the rock slope stability by combining a theoretical analysis and field tests. Lim *et al.* used the finite-element upper- and lower-bound limit analysis methods to investigate the three-dimensional (3D) slope stability (Lim *et al.* 2015). Johari and Javadi used the jointly distributed random variables method for a probabilistic analysis and reliability assessment of the stability of infinite slopes without seepage (Johari *et al.* 2012). Jackson *et al.* (2004) presented a methodology for mapping the theoretical factor of safety under earthquake loading using a conservative infinite slope model (Jackson *et al.* 2004). Hugues *et al.* (2014) presented a stability analysis of long and steep vegetated and barren slopes under saturated and seismic conditions and also evaluated the effectiveness of the infinite slope equation for these slopes (Hugues *et al.* 2014). However, such approaches based on a mechanical model can be complex and time-consuming and have two disadvantages: (a) failure to assess the slope stability in the absence of the geometry and soil properties pertaining to the formulation and (b) difficulty in representing practical conditions influenced by prior user assumptions (Cao *et al.* 2002, Ramin *et al.* 2017). Intelligent mathematical models analyze and forecast the slope behavior on the basis of the related monitoring and survey data. Taha *et al.* applied particle swarm optimization to calculate the minimum reliability index and critical probabilistic failure surface to evaluate the reliability of earth slopes and locate the critical probabilistic slip surface (Taha *et al.* 2014). Choobbasti *et al.* (2009) developed artificial neural network (ANN) systems consisting of multilayer perceptron networks to predict the slope stability in a specified location using several important parameters (Choobbasti *et al.* 2009). Kaunda *et al.* (2009) applied a back propagation neural network (BPNN) to three common challenges in engineering geology (Choobbasti *et al.* 2009, Tsai *et al.* 2017). Chok *et al.* (2016) investigated the feasibility of using ANNs to develop a random finite-element model to generate possible solutions and to

*Corresponding author, Ph.D.
E-mail: ymym_059@126.com

ISSN: 1225-4568 (Print), 1598-6217 (Online)

establish a large database (Kaunda *et al.* 2009). Suman *et al*. (2016) attempted to provide prediction model equations that can be used to predict the factor of safety of a slope by using artificial intelligence techniques (Chok *et al.* 2016). Such approaches based on intelligent mathematical models are referenced in this paper because they have simple operations and the following two advantages: (a) the ability to map complicated functional relationships between dependent and independent variables with few prior assumptions and control parameters and (b) the clear functional relations between the inputs and the outputs, implying a mathematical formulation of fundamental laws (Cao *et al.* 2002, Yang *et al.* 2017b).

The slope is divided into natural slope and artificial slope. The natural slope is gradually stabilized by weathering after unloading. The artificial slope is stabilized by reinforcement measures after cutting and excavating. For the unloading rock slope resulted from cut and excavation, it characterized by complex stress condition, sensitivity of disturbance and high deformation requirement. Unloading rock slope is a special and dangerous structural system, thus, it is extremely important to carry out research and analysis of its safety state.

At present, many scholars have extensively investigated the stability of an unloading rock slope over time and obtained an identified value rather than a range through such evaluations. The slope deformation properties change with the stress field under strong unloading so that the slope displacement monitoring data show obvious characteristics of nonlinear and nonstationary waves; thus, the prediction of the range of variation would be a much better fit in practice. BPNNs can acquire the characteristics and regularity of a historical sequence and predict the trend of the sequence. However, in a BPNN model, the initial weights and thresholds are randomly generated, and the lack of a basis can affect the sequence fitting. Genetic algorithms (GAs) follow the law of the survival of the fittest and choose an evolved individual as the optimal solution, such that it can overcome the shortcomings of BPNNs and improve the stability of the model. On this basis, to obtain the range of variation in a sequence over some time period, fuzzy information granulation (FIG) (Suman *et al.* 2016, Won *et al.* 2005, Li *et al.* 2009), which can partition the sequence and extract the characteristic parameters of every partition, is proposed and combined with a GA and BPNN. The FIG-GA-BPNN model can take full advantage of FIG for partition and information extraction, the GA for parameter optimization, and the BPNN for trend forecasting and finally predict the range of variation in the sequence. The FIG-GA-BPNN model is applied to predict the rock slope displacement sequence, and its accuracy is tested and verified.

2. GA-BPNN model for time-series fitting

2.1 Modeling principles of the BPNN model

The BPNN model is based on the back propagation algorithm, which is a type of gradient descent algorithm and is a supervised learning algorithm (Yu *et al.* 2013, Moon *et al.* 2010). A BPNN includes an input layer, an output layer, and a hidden layer. The learning process is divided into two phases. In the first phase, called the forward propagation stage, the input signal is processed from the input layer to the hidden layer and then to the output layer. The degree of activation of every neuron is determined by the input, an activation function, and a threshold. In the second phase, called the backward propagation stage, the output error is calculated and is propagated backward, and the weights and thresholds are corrected constantly so that the objective function of the error is minimized.

2.1.1 Forward propagation of information

The number of training samples is k; every training sample is composed of the input layer node set and the output layer node set. Here, $P = [p_1, p_2, \ldots, p_l]$ is the input layer node set, $S = [s_1, s_2, \ldots, s_m]$ is the hidden layer node set, and $A = [a_1, a_2, \ldots, a_n]$ is the input layer node set. The training samples are known, and random numbers are used as the initial weights and thresholds; therefore, the value of the i-th node in the hidden layer is

$$s_i = f^1\left(\sum_{j=1}^{l} p_j \times w^1_{i,j} + b^1_{si}\right) \tag{1}$$

where $w^1_{k,i}$ is the connection weight between the i-th node of the input layer and the kth node of the hidden layer, f^1 is the excitation function of the hidden layer, and b^1_{si} is the threshold of the kth neurons in the hidden layer, where $w^1_{i,j}$ and b^1_{si} are in the range from –1 to 1.

The value of the j-th node in the input layer is

$$a_i = f^2\left(\sum_{j=1}^{m} s_j w^2_{i,j} + b^2_{ai}\right) \tag{2}$$

where f^2 is the excitation function of the output layer, $w^2_{i,j}$ is the connection weight between the j-th neuron of the hidden layer and the i-th neuron of the output layer, and b^2_{ai} is the threshold of the i-th neuron in the output layer, where $w^2_{i,j}$ and b^2_{ai} are in the range from –1 to 1.

2.1.2 Backward propagation of error k samples are trained

The k input layer node sets of samples, which are l-dimensional vectors, are forward propagated to the hidden layer and then to the output layer to obtain the actual output values A. The actual output A and the expected output T are compared to calculate the root mean square error *RMSE*.

If *RMSE* does not meet the requirements, the process enters the backward propagation stage. The error signal is returned layer-by-layer with the formation of the gradient structure according to the previous path of a forward propagation stage. *RMSE* is allocated to all neurons in each layer to obtain $RMSE_j$ ($j = 1, 2, 3$) of each layer. $RMSE_j$ is considered as the basis for modifying the weights and threshold. Two phases are repeated until *RMSE* converges to the specified value.

For the above process, the BPNN can realize a nonlinear mapping from the input space to the output space. However, the initial weights, the initial thresholds, and the number of hidden layer nodes need to be determined, which is vital to the accuracy of the predicted results. The determination of the number of hidden layer nodes is often based on experience and experiments. In this study, the optimal number of hidden layer nodes is selected on the basis of a trial method in which the simulation error of the training samples is continuously improved through continuous testing and a continuous change in the number of hidden layer nodes. The optimization of the initial weights and thresholds is achieved by the GA and is described as follows.

2.2 Improved BPNN model based on a GA

A GA is a heuristic algorithm for solving the fast searching problem of optimal values. A GA pursues the production of new individuals better than existing individuals, which is the evolvability of the population (Jiang *et al.* 2014, Hu *et al.* 2015, Yang *et al.* 2015). First, this algorithm generates a set of populations, and the individuals in the populations are coded by two-dimensional coding. Then, the output values of each individual are calculated using the BPNN model, and the fitness values of all individuals are obtained. Furthermore, a search for evolving the current populations is implemented on the basis of selection, crossover, and mutation. The evolutionary principle is that a higher individual adaptability results in a higher probability of inheritance to the next generation. Multiple iterations are carried out until the expected error is reached. Finally, the fitness functions of each generation are obtained to obtain the optimal solution.

The individuals are composed of the weights and thresholds, and the individual length is

$$l = (s+1)t \tag{3}$$

where t is the number of hidden layer nodes, and s is the number of output layer nodes.

The operation is based on the roulette rule, in which the next-generation population is selected on the basis of the proportion of fitness. The cross operation is based on the real-coded crossover rule. The mutation operation involves the random selection of a new individual from a specified range to replace the original individual according to some probability.

The fitness function is the basis of an evolutionary search. The fitness function adopted in this study is

$$F = d\left(\sum_{i=1}^{n} abs(o_i - y_i)\right) \tag{4}$$

where n is the number of output layer nodes, o_i is the predicted value of the i-th node, y_i is the expected value of the i-th node, and d is the coefficient.

There are two termination conditions. The first is based on the fitness value. If the fitness value of an individual meets the expected value, the individual is the optimal individual. The other is based on the degree of convergence of the individual fitness value in the optimization process. Here, c is a specified value, and if the individuals in c successive generations have not changed, the calculation is terminated, and the optimal individual is selected as the final optimal individual. When the iteration result meets one of the above two conditions, the iteration can be stopped, and the solution corresponding to the optimal individual is output as the optimal solution.

The basic steps of the GA–BPNN model are summarized in Fig. 1.

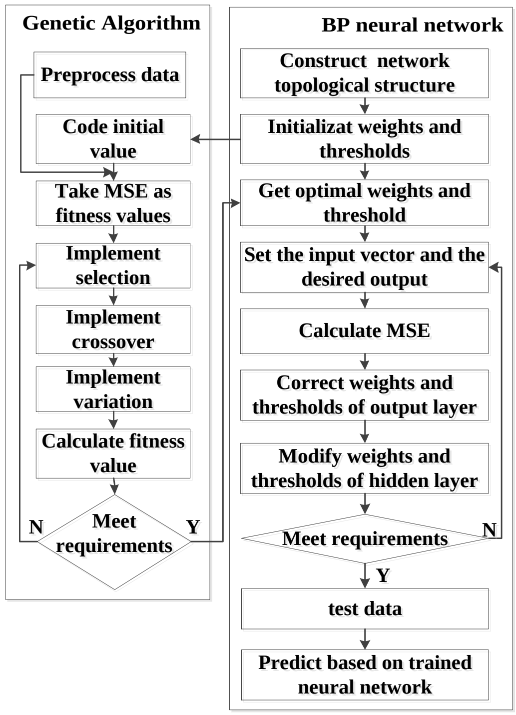

Fig. 1 Flow diagram of the GA–BPNN model

2.3 Time-series fitting based on the GA-BPNN model

A time series contains the information of the relevant influencing factors, and the GA-BPNN model can fit the earlier values of the time series to predict the later values.

To make full use of the latest information and improve the prediction accuracy, the rolling prediction method is used in the GA-BPNN model. For every example, its input layer node set is composed of the first l measured values, and the output layer node set of every example is composed of the latter n measured values. The time series consisting of p measured values can be divided into $p - l - n + 1$ trained examples. The prediction function is obtained by using the GA-BPNN model to train these examples. Then, the obtained prediction function predicts the future time series $\{o_{p-l+1}, o_{p-l+2}, \ldots, o_p\}$ using the input layer node set $\{y_{p+1}, y_{p+2}, \ldots, y_{p+n-1}\}$, and after obtaining the following n measured values, the model trains the measured time series $\{y_{n+p-l+1}, y_{n+p-l+2}, \ldots, y_{n+p}\}$ to predict the time value $\{o_{p+n+1}, o_{p+n+2}, \ldots, o_{p+2n-1}\}$ and so forth.

When the GA-BPNN model is established, the trial method is used to optimize the numbers of training steps, predicted steps, and hidden layer nodes. The steps are as follows.

Step 1. Establish the training samples and predicted samples according to all of the combinations of the different numbers of trained steps and predicted steps.

Determine the historical step h, predict the number of steps p, and establish the training time series and tested time series.

Step 2. Set the range of the number of hidden layer nodes and establish the GA-BPNN model on the basis of any value within the range.

Step 3. Calculate the fitness value.

Step 4. Compare the fitness values of the different combinations; the combination corresponding to the optimal fitness value is the optimal solution.

Step 5. Establish the optimal GA-BPNN model to train the historic time series to predict the trend of the time series.

Step 6. During rolling prediction, determine whether it is necessary to produce a new rule when adding a new data. According to the Eq. (4), the predicted value of the new data is calculated by the existing rule to obtain the current prediction error $RMSE_i$, which need to compare with critical error $RMSE_I$. If $RMSE_i \geq RMSE_c$, it shows that the previous rule can represent the new data. If $RMSE_i < RMSE_c$, it shows that the previous rule cannot represent the new rule and a new rule should be produced by returning to Step 2.

3. FIG-GA-BPNN model

3.1 Modeling principles of the FIG model

Professor L. A. Zadeh proposed the problem of FIG, which studies the performance characteristics of information partitions that are combinations of successive information granules. The displacement time series is extracted from the monitoring data at periodic intervals; thus, every element of the series is an information granule. In the process of slope creep, continuous information may contain redundant features; however, intermittent information may contain incomplete information. Thus, it is feasible to establish FIG, which can effectively extract the characteristics from intermittent information and the eliminate redundant features from continuous information (Shu *et al.* 2016, Ren *et al.* 2014, Yu *et al.* 2009, Ozer *et al.* 2011).

FIG mainly includes two steps: partitioning of a time series and fuzzifying the information of every part. In partitioning, the time series is divided into finite subsequence partitions. In the fuzzifying of information, the information of each subsequence part is fuzzified using a mathematical method so that the information of the subsequence parts can be described. The core of FIG is to construct a fuzzy granule P based on the time series $Y = \{y_1, y_2, ..., y_n\}$ or to establish a fuzzy concept G (a fuzzy set taking Y as the domain) that can reasonably describe Y. Here, P is determined by determining G; thus, the essence of the fuzzy process is the determination of the membership function A of G. First, the basic form of the fuzzy granule is determined; then, the specific membership function is determined. There are some types of commonly used forms of the membership function: triangular, ladder, Gaussian, parabolic, and so on.

Based on the fuzzy clustering algorithm of the displacement sequence, it is feasible to identity the characteristics of displacement and divide the displacement cluster. Thus, it is realized to make the fast modelling and accurate prediction for displacement on the basis of the consistency and historical feature of displacement.

To achieve good results and simplify the process, this study uses the ladder form of the membership function A that can be expressed as

$$A(x, up, r_1, r_2, low) = \begin{cases} 0, & x < low \\ \dfrac{x - low}{r_1 - low}, & low \leq x < r_1 \\ 1, & r_1 \leq x \leq r_2 \\ \dfrac{up - x}{up - r_2}, & r_2 \leq x \leq up \\ 0, & x > up \end{cases} \tag{5}$$

where x is the variables in the domain, and up, r_1, r_2, and low are the four characteristic parameters of the subsequence part.

There are two basic ideas for fuzzifying information. First, the characteristic parameters can reasonably represent the original data. Second, the characteristic parameters have some particularity. To meet and balance the two ideas, A can be expressed as follows

$$\begin{cases} M_A = \sum_{x \in X} A(x) \\ N_A = measure(supp(A)) \\ Q_A = \dfrac{M_A}{N_A} \end{cases} \tag{6}$$

where M_A meets the first basic idea, and N_A meets the second basic idea.

The steps for determining the four characteristic parameters are as follows.

Step 1. Determine r_1 and r_2.

In accordance with the small to large law, the time series $Y = \{y_1, y_2, \ldots, y_n\}$ is sorted to obtain the new sequence $Z = \{z_1, z_2, \ldots, z_n\}$. When n is an even number, $r_1 = z_{n/2}$, and $r_2 = z_{(n+2)/2}$. When n is an odd number, $r = r_1 = r_2 = z_{(n+1)/2}$.

Step 2. Determine low as follows

$$Maximize\, Q(a) = \frac{\sum_{x \leq r_1 \text{ and } x \in X} A(x)}{r_1 - low} \tag{7}$$

Step 3. Determine up as follows

$$Maximize\, Q(b) = \frac{\sum_{x \geq r_2 \text{ and } x \in X} A(x)}{up - r_2} \tag{8}$$

3.2 Time-series fluctuation-range prediction model based on the FIG-GA-BPNN model

Owing to the prominent advantages of FIG in granule-based information processing, this paper presents a time-series fluctuation-range prediction model based on the FIG-GA-BPNN model. The steps are as follows.

Step 1. Determine the partition size to partition the sample data and process it using FIG.

Step 2. Establish the GA-BPNN model for the time sequences that are combinations of the characteristic parameters of each subsequence part.

Step 3. Use the prediction models to predict the characteristic parameters of the next part.

Step 4. Analyze the predicted result.

4. Case study

The total reservoir capacity of a large hydropower station is 2.710×10^8 m^3, the normal water level is 900.000 m, the dead water level is 860.000 m, the retaining building is a concrete-faced rock-filled dam, and the maximum dam height is 115 m. There is a larger unloading area in the left bank from 865 to 960 m in height, which has an area of about 17380 m^2.

During the construction, the slope is treated in accordance with the principle of “cutting crest, reduce middle and supporting foot”. The slope is excavated above the height of 925 m, is reinforced by the combination with anchorage pile, anchor cable, anchor and drainage system at the height of 905-935 m and is confined by concrete and anchor cable below the height of 905 m. In addition, integrate rock is retained and the concrete cover is laid on the toe slab.

The strong-unloading rock slope was unstable, and several landsides occurred during construction. In January 2006, modification of the magnitude of the excavation slope and reinforcing and supporting measures comprising a combination of a slope to attach concrete, an anchor, and a pretensioned cable were completed. Then, the slope stability analysis results basically met the design requirements, and evident deformation was not found by site reconnaissance. However, taking into account the strong-unloading effect on the slope stability and considering that the strong-unloading slope is located in the abutment and the intake of the conduit system, the slope would cause a profound impact if it crashed. It is still necessary to improve the deformation monitoring of the slope, and the slope is displaced until slip occurs, which is a continuous and lengthy process. For this reason, the deformation of the slope is monitored, and data are regularly collected on the left bank of the unloading rock slope. The process from slipping to failure is continuous and long. In practical engineering, a multipoint displacement meter is arranged to monitor the deformation of the slope over a long time, and the monitoring data are collected regularly. The slope system is shown in Fig. 2.

The initial impoundment process of the reservoir is as follows. Closure began in February 2005. Impounding of the reservoir started in October 2007. The first generating unit of power went online in April 2008. During this period, the water levels were lower than the dead water level and were lower than the strong-unloading area. Thus, the fluctuation in the reservoir level did not affect the deformation of the slope. The deformation of the slope is basically caused by aging so that the tendency of the variation in the displacement can be predicted by a fitted historical time series. The monitoring data of the C2-XH-M-02 displacement monitoring point are used in this study. This study utilizes 78 measured values collected once about every 10 days from January 22, 2006 to March 22, 2008. Thirty-six values collected earlier are taken as training samples, and 42 values collected later are used for comparison with the predicted values to evaluate the prediction performance of the model.

To confirm the accuracy of the model presented in this paper, the five indexes in Table 1 are used to analyze the predicted result.

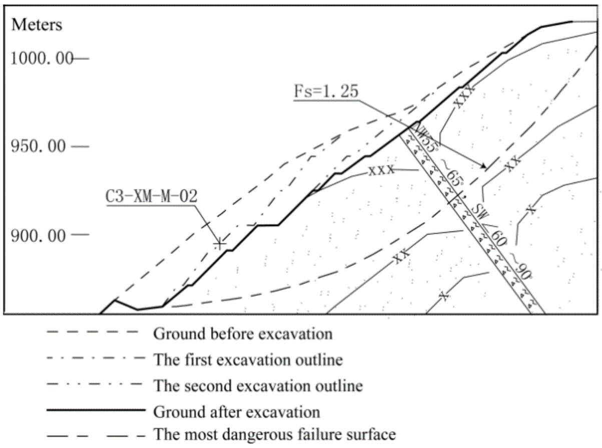

Fig. 2 Slope system

Table 1 Simulation performance indexes

Index	Calculation formula
Root mean square error	$RMSE=\sqrt{\sum_{i=1}^{s}\frac{[o_i-y_i]^2}{(s-1)}}$
Mean absolute percentage error	$MAPE=\frac{1}{s}\sum_{i=1}^{s}\left\lvert\frac{o_i-y_i}{o_i+y_i}\right\rvert$
Normalized mean square error	$NMSE=\frac{\sum_{i=1}^{s}[o_i-y_i]^2}{\sum_{i=1}^{s}[y_i-\bar{y}]^2}$
Mean absolute value of prediction error	$MAVPE=\frac{1}{s}\sum_{i=1}^{s}\lvert o_i-y_i\rvert$
Maximum absolute value of prediction error	$MAXAVPE=\max(\lvert o_i-y_i\rvert)$

4.1 Comparison between the GA-BPNN and BPNN models

To reinforce the arguments presented in this paper, the BPNN and GA-BPNN models are established to demonstrate the superiority of the GA-BPNN model over the BPNN model.

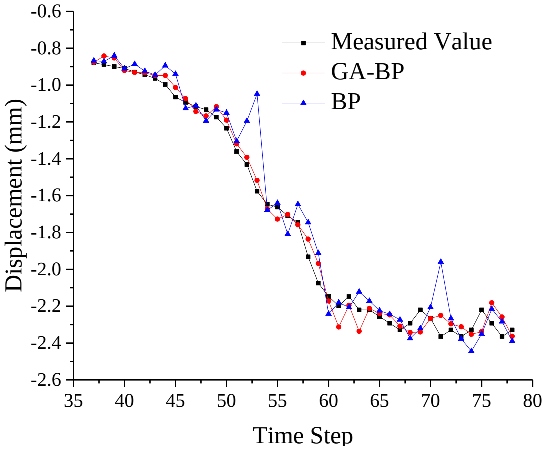

Fig. 3 Predicted values obtained by different models and the actual values

Table 2 Comparison of the simulated performance of two prediction models

Model	Performance index				
	RMSE	*MAPE*	*NMSE*	*MAVPE*	*MAXAVPE*
BPNN model	0.1269	0.0255	0.0495	0.0845	0.52 78
GA–BPNN model	0.0627	0.0139	0.0121	0.0499	0.12 05

For the GA, according to experience, the number of populations is set to 20, the number of maximum genetic algebras is set to 100, the crossover probability is set to 0.7, the mutation probability is set to 0.01, and the generation gap is set to 0.95. For the BPNN, according to the trial method, the numbers of input layer nodes, hidden layer nodes, and output layer nodes are 6, 14, and 1, respectively. On the basis of the above preset parameter values, the GA–BPNN and BPNN models are established. It is found that the fitness values of the BPNN model have leveled off before 100 iterations; however, the fitness values of the GA-BPNN model have leveled off before 50 iterations. The final fitness values of the GA-BPNN model are better than those of the BPNN model.

The results predicted by the two models are presented in Fig. 3 and Table 2.

The results in Fig. 3 show that the predicted values of GA-BP model are closer to measured values than BP model. The results in Table 2 show that, the values of *RMSE*, *MAPE*, *NMSE*, *MAVPE* and *MAXAVPE* of the GA-BPNN model is reduced by -50.6%, -45.5%, -75.6%, -40.9% and -77.2% respectively by comparing the BPNN model. The predicted results show that the optimization of the initial weights and thresholds has a major influence on the prediction accuracy of the model. The GA-BPNN model is superior for the prediction of a time series to the BPNN model.

4.2 Prediction performance analysis of the GA-BPNN model

Displacement slippage is a continuous process. In practical engineering, iterative multistep prediction without changing the model is necessary to arrange the management and maintenance of the slope earlier. Iterative multistep prediction means that a later value is predicted by adding the first predicted value.

Denoting the number of prediction steps by L and the number of values that need to be predicted by K, the number of established prediction models is $\lceil K/L \rceil$. The results for different iterative multistep predictions are presented in Fig. 4 and Table 3.

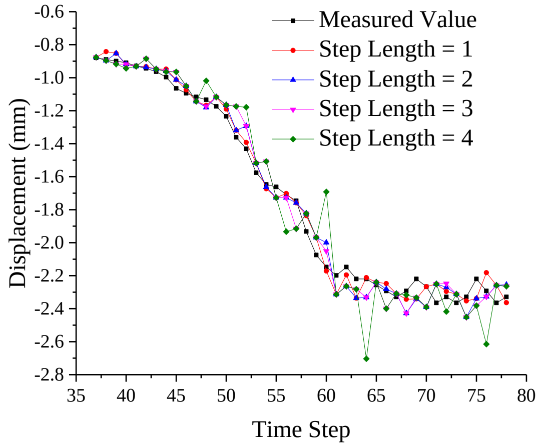

Fig. 4 Predicted values obtained by different multistep prediction models and the actual values

Table 3 Comparison of the simulated performance of different multistep prediction models

Number of prediction steps	Index				
	RMSE	*MAPE*	*NMSE*	*MAVPE*	*MAXAVPE*
1	0.0627	0.0139	0.0121	0.0499	0.1205
2	0.0771	0.0170	0.0183	0.0629	0.1477
3	0.0897	0.0210	0.0248	0.0754	0.1875
4	0.1464	0.0288	0.0660	0.1052	0.4832

The results in Fig. 4 show that predicted results show that the predicted curve is close to the actual curve. However, as the number of prediction steps increases, errors accumulate. The results in Table 3 show that by comparing the one-step prediction, the values of *RMSE*, *MAPE*, *NMSE*, *MAVPE* and *MAXAVPE of* two-step prediction is increased by 23.0%, 22.3%, 51.2%, 26.1% and 22.6% respectively; the values of *RMSE*, *MAPE*, *NMSE*, *MAVPE* and *MAXAVPE of* three-step prediction is increased by 43.1%, 51.1%, 105.0%, 51.1%, and 55.6% respectively; the values of *RMSE*, *MAPE*, *NMSE*, *MAVPE* and *MAXAVPE of* three-step prediction is increased by 133.5%, 107.2%, 445.5%, 110.8%, 301.0% respectively.

It is obvious that the errors of the iterative four-step prediction model are greater than the other models, and the prediction accuracy is difficult to guarantee. To obtain the ideal result, the number of prediction steps should not exceed 3.

4.3 Analysis of the FIG-GA-BPNN model

For the above process of modeling forecasting, the

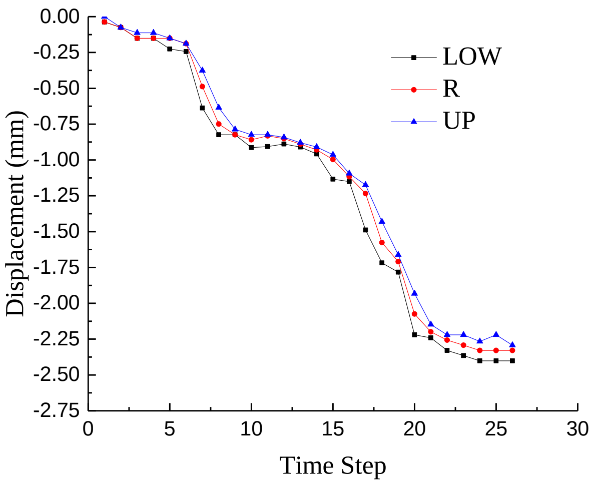

Fig. 5 Characteristic parameters of all partitions based on FIG

Table 4 Mean error comparison between the actual and predicted values

Time series	Index				
	RMSE	*MAPE*	*NMSE*	*MAVPE*	*MAXAVPE*
LOW	0.0481	0.0065	0.0218	0.0239	0.1521
R	0.0387	0.0053	0.0139	0.0178	0.1319
UP	0.0470	0.0073	0.0212	0.0245	0.1215

variation in the displacement has a periodic feature where the displacement rapidly increases in steps and slowly increases or fluctuates within a phase. Thus, the prediction of the range of variation of a time series is in greater agreement with the actual conditions. Considering the above predicted results, the division of a time series into partitions every three consecutive data points in the FIG-GA-BPNN model is most suitable.

According to FIG theory, the 78 measured displacement values are divided into 28 partitions, and the characteristic parameters of all partitions are obtained. The characteristic parameters of all partitions form the characteristic-parameter time sequences *LOW*, *R*, and *UP*, where $LOW = [low_1, low_2, \ldots, low_{28}]$, $R = [r_1, r_2, \ldots, r_{28}]$, and $UP = [up_1, up_2, \ldots, up_{28}]$. The characteristic parameters of the first 12 partitions are taken as training samples. The characteristic parameters are shown in Figure 5.

The characteristic parameters of the latter 16 partitions are used for comparison with the predicted values to evaluate the prediction performance of the FIG-GA-BPNN model. The predicted results for *LOW*, *R*, and *UP* are presented in Fig. 6 and Table 4.

The predicted results show that the displacement values increase in steps and become increasingly gentle. It follows that the position where the displacement monitoring point is placed is stable. In addition, post in-site monitoring verifies the predicted results that the deformation of the slope tends to level off and the rock mass tends to be stable. Comparing the measured and predicted values, the results show that the values of *MAVPE* for *LOW*, *R*, and *UP* are 0.0239, 0.0178, and 0.0245, respectively. These values of *MAVPE* are far lower than the average of the measured values. Moreover, other prediction performance indices indirectly indicate that the predicted results are in accordance with the actual accident situation. On the basis of the above analysis, the results predicted by the FIG-GA-BPNN model meet engineering requirements. It is further verified that the FIG-GA-BPNN model has a forward effect on the prediction of the displacement of a strong-unloading rock slope and can be applied to engineering.

For the BPNN model, the value of RMSE is 0.1269, the value of MAPE is 0.0255, the value of NMSE is 0.0495, the value of MAVPE is 0.0845, and the value of MAXAVPE is 0.5278. For the GA-BPNN model, the value of RMSE is 0.0627 decreasing by 50%, the value of MAPE is 0.0139 decreasing by 45%, the value of NMSE is 0.0121

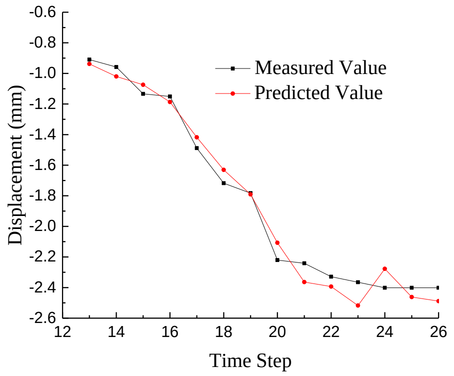

(a) *LOW*

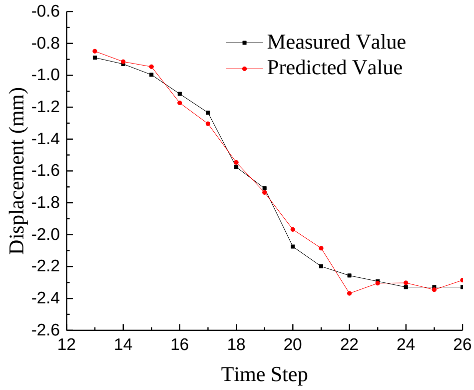

(b) *R*

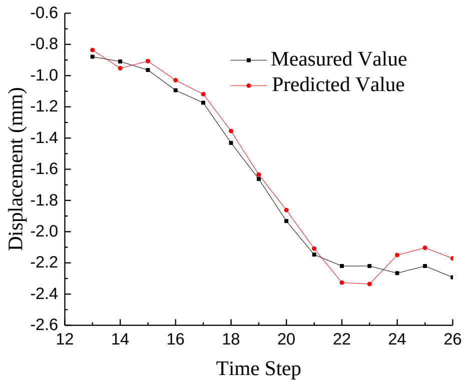

(c) *UP*

Fig. 6 Predicted and actual values of the characteristic parameters in partitions decreasing by 76%, the value of MAVPE is 0.0499 decreasing by 41%, and the value of MAXAVPE is 0.1205 decreasing by 77%. The prediction results show that the optimization of initial weights and thresholds has a great influence on the prediction accuracy of the model. GA-BPNN model is superior in prediction of a time series to the BPNN model.

5. Conclusions

This study presents the FIG-GA-BPNN model to predict the range of variation in the strong-unloading rock slope on the basis of monitoring data. The following conclusions were found.

(a)The GA-BPNN model was established by combining the properties of a BPNN to fit a time series and the properties of a GA to optimize the initial weights and initial thresholds of the BPNN. When using the GA-BPNN model to fit a time series, the optimal numbers of hidden layer nodes, input layer nodes, and output layer nodes are determined by a trial method based on the prediction error. The GA-BPNN model can retain the ability to learn using training samples and avoid the random selection of the initial parameters, which makes the GA-BPNN model an invaluable tool in time-variant problems such as creeping landslides or earth slumps.

(b)The FIG model can partition a time series and extract the characteristic parameters from every partition, and the GA-BPNN model can fit any nonlinear function. Combining the advantages of these two models, the FIG-GA-BPNN model can effectively predict the range of fluctuation in the time series.

(c)A practical case shows that the FIG-GA-BPNN model can extract the evolution information of the slope from the displacement time series to predict the future range of variation in the displacement of the slope by continuous iteration.

(d)The FIG-GA-BPNN model provides a basis for evaluating the slope stability and has contributed to the prediction and warning of slope disasters. This model can be applied to the field of slope displacement prediction and provide new ideas for other areas of forecasting modeling.

Acknowledgments

The research described in this paper was financially supported by the Project of National Natural Science Foundation of China/Yalong River Joint Fund (Grant No. U1765205), the Innovation Research Project for Postgraduate in Jiangsu Province (KYZZ16_0284), a Project Funded by the Priority Academic Program Development of Jiangsu Higher Education Institutions (PAPD)(YS11001), the Project of National Natural Science Foundation of China (Grant No. 51609073), and the Fundamental Research Funds for the Central Universities(Grant No. 2016B04114).

References

Cao, J. (2002), "Neural network modeling and analytical modeling of slope stability", Ph.D. Dissertation, University of Oklahoma, U.S.A.

Chen, S.S., Fu, Z.Z., Wei, K.M. and Han, H.Q. (2016), "Seismic responses of high concrete face rockfill dams: A case study", *Water Sci. Eng.*, **9**(3), 195-204.

Chok, Y.H., Jaksa, M.B. and Kaggwa, W.S. (2016), "Neural network prediction of the reliability of heterogeneous cohesive slopes", *Int. J. Numer. Anal. Met.*, **40**(11), 1556-1569.

Choobbasti, A.J., Farrokhzad, F. and Barari, A. (2009), "Prediction of slope stability using artificial neural network (case study: Noabad, Mazandaran, Iran)", *Arab. J. Geosci.*, **2**(4), 311-319.

Choobbasti, A.J., Farrokhzad, F. and Barari, A. (2009), "Prediction of slope stability using artificial neural network (case study: Noabad, Mazandaran, Iran)", *Arab. J. Geosci.*, **2**(4), 311-319.

Hu, W. and Cao, W. (2015). "Slope stability evaluation based on hybrid algorithm of particle swarm optimization and BP neural network", *J. Rail Way Sci. Eng.*, **12**(1), 66-71.

Hugues, G., Claude, P. and Jean-Claude, V. (2014), "A suitable methodology for assessing impacts of successive rainfalls infiltration on road slope stability", *Acta Geotech.*, **9**(5), 753-770.

Jackson, R., Gunn, D.A. and Long, D. (2004), "Predicting variability in the stability of slope sediments due to earthquake ground motion in the AFEN area of the western UK continental shelf", *Mar. Geol.*, **213**(1-4), 363-378.

Jiang, S.H., Li, D.Q., Zhang, L.M. and Zhou, C.B. (2014), "Slope reliability analysis considering spatially variable shear strength parameters using a non-intrusive stochastic finite element method", *Eng. Geol.*, **168**, 120-128.

Johari, A. and Javadi, A.A. (2012), "Reliability assessment of infinite slope stability using the jointly distributed random variables method", *Sci. Iran.*, **19**(3), 423-429.

Kaunda, R.B., Chase, R.B., Kehew, A.E., Kaugars, K. and Selegean, J.P. (2010), "Neural network modeling applications in active slope stability problems", *Environ. Earth. Sci.*, **60**(7), 1545-1558.

Li, W. and Liu, L. (2009), "Application of fuzzy neural network for predicting natural slope failure due to underground mining in mountainous areas", *Fuzzy Syst. Math.*, **23**(3), 170-174.

Lim, K., Li, A.J. and Lyamin, A.V. (2015), "Three-dimensional slope stability assessment of two-layered undrained clay", *Comput. Geotech.*, **70**, 1-17.

Mendjel, D. and Messast, S. (2012), "Development of limit equilibrium method as optimization in slope stability analysis", *Struct. Eng. Mech.*, **41**(3), 339-348.

Moon, H. (2010), "The prediction of rock slope stability in Korea using artificial neural network", *J. Kor. Soc. Min. Energy Res. Eng.*, **47**(1), 31-44.

Nieuwenhuis, J.D. (1991), "The lifetime of a landslide: Investigations in the French alps", *A. A. Balkema, Rotterdam*, 144.

Ozer, M. (2011), "An application of fuzzy information granulation in the emerging area of online sports", *Exp. Syst. Appl.*, **38**(4), 4514-4521.

Ramin, T.M. (2017), "Seismic response of soil-structure interaction using the support vector regression", *Struct. Eng. Mech.*, **63**(1), 115-124.

Ren, C., Liang, Y. and Pang, G. (2014), "The empirical mode decomposition and genetic algorithm-wavelet neural network for slope deformation prediction research", *J. Geomat. Sci. Technol.*, **31**(96), 551-555.

Shu, S. and Gong, W. (2016), "An artificial neural network-based response surface method for reliability analyses of c-phi slopes with spatially variable soil", *Chin. Ocean Eng.*, **30**(1), 113-122.

Su, H., Yang, M. and Wen, Z. (2016), "An approach using multi-factor combination to evaluate high rocky slope safety", *Nat. Hazard. Earth Syst.*, **16**(6), 1449-1463.

Suman, S., Khan, S.Z. and Das, S.K. (2016), "Slope stability analysis using artificial intelligence techniques", *Nat. Hazard.*, **84**(2), 727-748.

Taha, M., Khajehzadeh, M. and El-Shafie, A. (2012), "Application of particle swarm optimization in evaluating the reliability of soil slope stability analysis", *Sains Malays.*, **41**(7), 847-854.

Tsai, P., Ahmad, H.B. and Chen, C. (2017), "Structural system simulation and control via NN based fuzzy model", *Struct. Eng. Mech.*, **56**(3), 385-407.

Won, P. (2005), "Stavility evaluation of the cut slope using artificial neural network model", *J. Kor. Soc. Civil Eng.*, **25**(4C), 275-283.

Yang, H., Xie, S., Secq, J. and Shao, J. (2017a), "Experimental study and modeling of hydromechanical behavior of concrete fracture", *Water Sci. Eng.*, **10**(2), 97-106.

Yang, M., Su, H. and Wen, Z. (2017b), "An approach of evaluation and mechanism study on the high and steep rock slope in water conservancy project", *Comput. Concrete*, **19**(5), 527-535.

Yang, M., Su, H. and Yan, X. (2015), "Computation and analysis of high rocky slope safety in a water conservancy project", *Discr. Dyn. Nat. Soc.*, 197579.

Yu, F.S. and Pedrycz, W. (2009), "The design of fuzzy information granules: Tradeoffs between specificity and experimental evidence", *Appl. Soft Comput.*, **9**(1), 264-273.

Yu, W., Cai, J. and An, F. (2013), "On slope displacement prediction model based on lmd-bp neural network", *Comput. Appl. Softw.*, **30**(9), 107-109.

Zhang, Y., Xu, W., Shao, J., Zhao, H. and Wang, W. (2017), "Experimental investigation of creep behavior of clastic rock in Xiangjiaba hydropower project", *Water Sci. Eng.*, **8**(1), 55-62.

CC